

## Numerical Analysis of the Crashworthiness Performance of Multicell Tubes Under Oblique Loads

Quirino Estrada<sup>1\*</sup>, Jarosław Zubrzycki<sup>2</sup>, Elva Reynoso<sup>1</sup>, Julio Vergara<sup>3</sup>,  
Aztlán Bastarrachea<sup>4</sup>, Alejandro Rodriguez-Mendez<sup>5</sup>, Manuel de Jesús Nandayapa<sup>1</sup>,  
Jesús Silva<sup>1</sup>, Francisco Enriquez Aguilera<sup>1</sup>, Lara Wiebe<sup>1</sup>

<sup>1</sup> Instituto de Ingeniería y Tecnología, Universidad Autónoma de Ciudad Juárez (UACJ), Ciudad Juárez, Chihuahua, México

<sup>2</sup> Mechanical Engineering Faculty, Lublin University of Technology, ul. Nadbystrzycka 38D, 20-618 Lublin, Poland

<sup>3</sup> Unidad Profesional Interdisciplinaria de Ingeniería, Campus Palenque (UPIIP)/IPN, Palenque, Chiapas, México

<sup>4</sup> Departamento de Ciencias Básicas, Tecnológico Nacional de México campus Ciudad Juárez, Ciudad Juárez, Chihuahua, México

<sup>5</sup> Tecnológico Nacional de México campus Ciudad Guzmán, Ciudad Guzmán, Jalisco, México

\* Corresponding author's e-mail: [quirino.estrada@uacj.mx](mailto:quirino.estrada@uacj.mx)

### ABSTRACT

When a car crash occurs, the probability that the collision will be oblique and not entirely frontal is high. In this way, the current article evaluates by a finite element analysis, the crashworthiness performance of multicell structures subjected to oblique loads. In this sense, five multicell structures manufactured with 6063-T5 aluminum alloy were designed and evaluated by an oblique compression test. During the analysis, special emphasis was placed on determining the effect of the cross-section and the angle of incidence of the load ( $\theta$ ) on the energy absorption of the structures. For this purpose, values of  $\theta$  equal to  $0^\circ$ ,  $5^\circ$ ,  $10^\circ$  and  $15^\circ$  were analyzed. To guarantee a correct comparison between tubes, all the structures had the same mass equal to 0.80 kg. Then, adjustments to the thickness were realized. In all cases, the most important indicators of impact resistance such as energy absorption ( $E_a$ ), crushing force efficiency (CFE), and mean force ( $P_m$ ) were calculated. According to the results, the angle of incidence of the load defined the plastic deformation mode of the structure. In this sense, a 47.75% decrease in the  $P_{max}$  and  $P_m$  was observed as the angle  $\theta$  increased. Moreover, at the end of the study, the MC-02 profile presented the best CFE with an average value of 0.74 at different loading angles. Thus, this structure could be considered as a baseline among engineers and designers for the design of structures subjected to bending loads.

### INTRODUCTION

The Crashworthiness concept is one of the most critical concepts in automobile industry [1]. In this way, body-in-white is designed to withstand the dynamic forces during car crashes, saving the integrity of the passengers. Car crashes occur in different directions, however, according to [2] statically frontal and oblique crashes represent 34% of all reported accidents. With this in mind, the use of thin-walled structures as an energy absorption mechanism is studied

by engineers and academics [5,6]. For the specific case of structures loaded obliquely, theoretical [3,4], experimental [7-8], and numerical [9,10] studies have been performed focusing on maximizing their plastic deformation. The main parameters analyzed are the geometric pattern, manufacture material, and the loading angle ( $\theta$ ). In this way, Karantza et al. [11] numerically and experimentally investigated the impact resistance of square aluminum profiles subjected to oblique loads. During the study, special emphasis was set on the variation of the load incidence angle

and its effect on the contact and initial deformation mode of the profile. They concluded that the energy absorption ( $E_a$ ) capabilities are improved meanwhile a decrease of the peak load ( $P_{max}$ ) is obtained when an initial contact with a corner is present. Davoudi et al. [12] conducted a study to evaluate the effect of the geometric shape of the profile and the angle of incidence of the load on the energy absorption performance of thin-walled structures. The profiles analyzed were polygonal with a tendency to form a circumference, and the angles of incidence of the load were from  $0^\circ$  to  $15^\circ$ . From their study, they determined that square and hexagonal structural profiles decreased their  $E_a$  capacity as  $\theta$  increased. Zhang et al. [13] computationally and experimentally analyzed the mechanical behavior of square tubes with thickness variations when subjected to oblique loads. During the analysis, three different thickness conditions were evaluated, as well as load incidence angles of  $0^\circ$ ,  $10^\circ$ , and  $15^\circ$ . The results revealed a better behavior of the profiles with graduated thickness than the conventional tube (uniform thickness). Liu, W. et al. [14] realized a multi-objective optimization analysis of star-shaped conical tubes under oblique impact loads. At the end of their analysis, they determined that the conical tubes with a concave fluted curve presented a better performance. In this sense, the specific energy absorption was increased by 9.87%. Tian et al. [15] carry out a numerical and experimental analysis to improve the energy absorption capacities of tubes under axial loads. For this purpose, in the study, slots with non-uniform depth in the circular profiles were drilled. The results showed the effectiveness of the non-uniform slots in increasing the  $E_a$  capacity. On the other hand, Rogala & Gajewski [16] numerically analyzed the mechanical performance of porous materials to be loaded obliquely. For this purpose, aluminum and PET foams were used. The analysis consisted of locating the foam on a base with a variable angle of inclination. The inclination angles evaluated were 15, 30, 45, and 60 degrees. The compression tests were carried out quasistatically and dynamically. In conclusion, they determined a similar energy efficiency for all the foams loaded quasistatically, meanwhile, in the dynamic case the PET foam absorbed up to 15 percent more energy. Li et al. [17] analyzed, numerical and experimentally, the crushing performance of hierarchical hexagonal tubes subjected to oblique impacts. During the research, impact angles of  $0^\circ$ ,

$10^\circ$ ,  $20^\circ$ ,  $30^\circ$  and  $40^\circ$  were studied. At the end of the study, the importance of the number of cells of the structure in the deformation mode was verified. Likewise, the best energy absorption performance was computed when the hierarchical structures were impacted at  $10^\circ$ . Alkhatib et al. [18] performed a numerical analysis to assess the crushing behavior of corrugated tapered tubes (CTTs) under oblique impact. For this purpose, several CTTs were impacted at seven oblique load conditions. As conclusion, they determined a 54% decrease in energy absorption as the impact angle increased from  $0$  to  $40^\circ$ . Moreover, the global bending mechanism was mostly visible for higher angles such as  $80^\circ$ . Similarly, Fan et al [19] performed an experimental and numerical crashworthiness analysis of metal composite thin-walled structures with holes subjected to axial and oblique loads. The load was applied to angles of  $0^\circ$ ,  $10^\circ$ ,  $20^\circ$  and  $30^\circ$ . According to their results, as the load angle increased, a decrease of energy absorption was observed. The opposite effect was observed for  $0^\circ$ , where an improvement of  $E_a$  was computed.

In conclusion, as presented in the previous state-of-the-art review, the study of thin-walled structures under oblique loads is relevant. However, the specific case of multicell tubes is barely reported. Thus, in the current paper, the crashworthiness performance of multicell tubes under oblique loads is presented. To reach this goal five multicell structures based on square shape were performed numerically using Abaqus finite element software. In all cases, the structures were manufactured with aluminum 6063-T5. During the analysis, special emphasis was set on the loading angle ( $\theta$ ) and its effect on crashworthiness performance. For this purpose, values equal to  $0^\circ$ ,  $5^\circ$ ,  $10^\circ$ , and  $15^\circ$  were studied.

### Mechanical characterization of aluminum 6063-T5

Aluminum alloys are widely used in the automotive industry due to their excellent relation between strength and weightless. With this in mind, aluminum alloy 6063-T5 was used as a manufacturing material for the structures in the current article. The mechanical characterization of the material was carried out by tensile tests based on ASTM/E8 [20]. This was performed by a Shimadzu AG-X plus 100kN universal test machine with a quasi-static velocity of 6 mm/min.

The accuracy and feasibility of the results were guaranteed since 3 tests were carried out. The obtained results are presented in Figure 1 where details of the true stress vs true strain are displayed. Likewise, the obtained mechanical properties are shown in Table 1.

### Experimental validation of a numerical compression test model

The current analysis is in numerical way. Thus, a first discrete model was developed in Abaqus/explicit and experimentally validated. The experimental setup consisted of a compression test of a square aluminum tube executed by a Shimadzu AG-X plus 100kN universal test machine at 6 mm/min and a axial loading angle ( $\theta$ ) of  $0^\circ$ . This condition is valid for our analysis of oblique load since future simulations are a special case of the crushing process with a variation of loading angle. The square profile has dimensions of  $38.1\text{mm} \times 38.1\text{mm} \times 130\text{mm}$  and a thickness ( $t$ ) of 1.5 mm. Respect to discrete model the tube was modeled with S4R (quadrilateral four-node shell element with reduced integration) and conferred with elastoplastic properties for Al 6063-T5. During the simulation the structure was compressed by two rigid plates which were modeled as 3D rigid elements for with four nodes (R3D4).

The contact condition between elements was guaranteed by a general contact interaction with  $\mu = 0.15$  [21]. Concerning boundary conditions, the upper plate was unconstrained only in y-direction meanwhile bottom plate was fully restricted. Lastly, from a mesh convergence analysis, an element size of 3 mm was implemented. Details of the discrete model are presented in Figure 2.

The obtained results both numerical and experimental models are presented in Figure 3-4. In this sense, Figure 3a presents the mechanical behavior of the crushing load along the displacement (80 mm). In both cases, the curves are characterized by an initial peak load ( $P_{max}$ ) close to 36 kN. Later, the failure of the tube is reached which can be observed as a sudden drop of the crushing force. From this point, the forming process of plastic wrinkles is initiated with smaller oscillations of crushing load. On the other hand, Figure 3b shows the absorbed energy ( $E_a$ ) by plastic deformation. In this case, a total  $E_a$  equal to 1.05 kJ was calculated. Likewise, the final deformation mode for both models is presented in Figure 4, where the discrete model reproduces correctly the form and number of plastic wrinkles. Finally, from minor differences of less than 5%, the discrete model was validated, allowing in this way, to continue with the numerical study of multicell squares tubes under oblique loads.

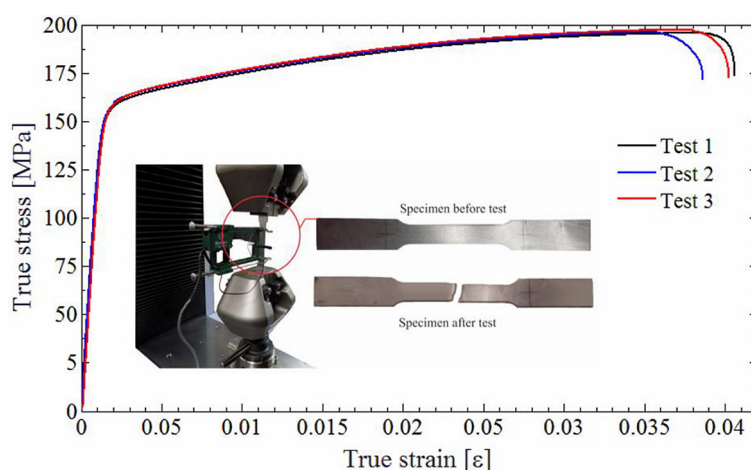
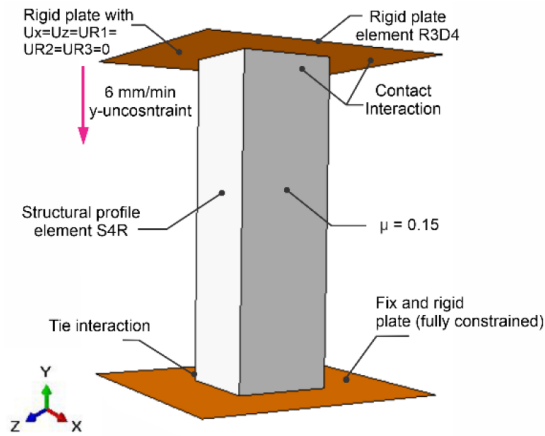


Fig. 1. True strain vs stress curves for aluminum 6063-T5 and experimental setup

Table 1. Elasto-plastic mechanical properties for aluminum 6063-T5

Elasticity	Young modulus [MPa]	Poisson coefficient	Density [kg/m <sup>3</sup> ]
	66940	0.33	2700
Isotropic plasticity model	Yield stress $S_y$ [MPa]		
	158.79		



**Fig. 2.** Boundary conditions for the axial compression test of the aluminum square profile

### Numerical simulations of multicell structures subjected to oblique loads

Since there is a high probability that car crashes occur in a frontal oblique way, the main purpose of this article is to evaluate the crashworthiness performance of multicell tubes subjected to different loading angles ( $\theta$ ). For this purpose, five multicell structures based on a square pattern were numerically analyzed by a quasistatic crushing test at 6 mm/min. In all cases, the structures were conferred with mechanical properties for aluminum alloy 6063-T5 and modeled with S4R elements. Likewise, the same mass equal to 80 gr was kept. To get a better understanding of the effect of loading angle, values of  $\theta$  equal to  $0^\circ$ ,  $5^\circ$ ,  $10^\circ$ , and  $15^\circ$  were analyzed. The loading angles were imposed through the orientation of the upper rigid plate concerning the horizontal axis. In this case, compression plates were modeled with C3RD rigid elements. With respect to boundary

conditions, the lower tip of the structures was attached to the bottom plate by a tie condition, while the upper plate was free to move only in y-direction and was constrained in all rotation degrees to maintain a constant loading angle. The contact interaction between profiles was guaranteed by a general contact  $\mu = 0.3$ . Lastly, the geometrical characteristics of the multicell thin-walled structures are presented in Table 2.

### RESULTS AND DISCUSSION

Upon completing the numerical simulations of the multicell structures their mechanical behavior was obtained by the curves of the force vs displacement curves. As a baseline for comparison purposes, the numerical results for a typical square tube (ST-00) are also presented. Figure 5 presents the mechanical behavior for each profile as well as each loading angle analyzed ( $0^\circ$ ,  $5^\circ$ ,  $10^\circ$  and  $15^\circ$ ). Regardless of the structure analyzed, as the loading angle ( $\theta$ ) decreases, the load-carrying capacity also diminishes. The behavior

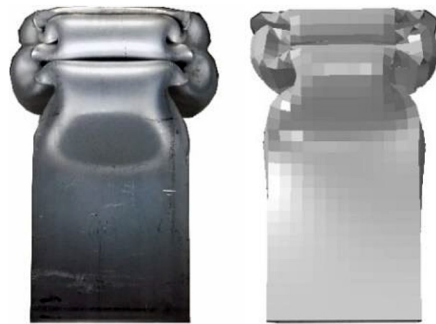


**Fig. 4** Comparison of the final deformation mode between experimental and numerical models

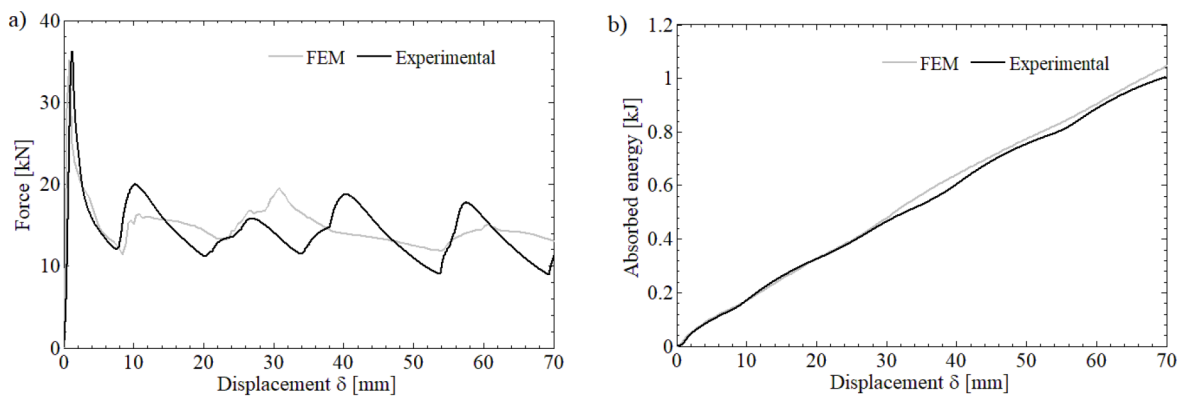


**Fig. 3.** (a) Force vs displacement and (b) energy absorbed vs displacement of both numerical and experimental results

**Table 2.** Geometric characteristics of multicell and typical structures, where a is equal to 38.1 mm

Specimen code	Length (mm)	Thickness (t)	Mass (g)
ST-00	130	1.50	80
MC-01	130	0.90	80
MC-02	130	1.00	80
MC-03	130	0.98	80
MC-04	130	0.98	80
MC-05	130	1.09	80

of the curves in all cases was determined by an initial increase of the crushing load until reaching a  $P_{max}$  value. Depending on the  $\theta$  value, the increase of load can be smoother as  $\theta$  increases. Reaching the  $P_{max}$  value, the effect of the geometry of the profile becomes important. In this case, depending on structural stability provided by the cross-section shape of the tubes, the forming of plastic wrinkles or failing that buckling effect appears along the crushing process. As expected, the buckling effect appears to a greater extent when the structures are loaded at  $15^\circ$ . Considering  $10^\circ$  and  $15^\circ$  the poorest mechanical behavior among multicell structures and the typical square was computed for structure MC-03 where a sudden drop the force at 25 mm up to reach a crushing force close to 2.5 kN was computed. However, the cross-section formed by a main square with smaller squares at the corners (MC-02) exhibited a better load carry capacity in all loading angles. This meant a greater stability of the structure.

The collapse mode for each assessed structure is shown in Figure 6. For all cases, the forming of static and traveling plastic hinge lines was mostly visible at  $0^\circ$  and  $5^\circ$ . This allowed the forming of higher numbers of bulges along the length of the tubes. In the opposite case, when

the structures were loaded at  $15^\circ$  a buckling effect was mostly observed. This phenomenon was observed to a greater extent for structure MC-03 and typical square tube (ST-00). For the case of a loading angle of  $10^\circ$  the structures experienced a mixed deformation mode characterized by the forming of plastic wrinkles at the top tip of the tubes, followed by buckling effect. For this loading angle, the cross-sections of structures MC-04 and MC-05 allowed to counteract the apparition of the buckling effect. On the other hand, particular torsional effects were also observed. Focusing on the multicell structure MC-02, the torsional effect contributed to forming plastic wrinkles with hinge lines in the direction of the transversal axis of the tube, which provided better stability of the structure when  $\theta$  is equal to  $10^\circ$  and  $15^\circ$ .

Many parameters are calculated for the crashworthiness analysis of the structures; however, the most important indicators are the peak load ( $P_{max}$ ) obtained directly from the curve, mean force ( $P_m$ ), absorbed energy ( $E_a$ ), and the crush force efficiency (CFE) which are independent of shape, material among others. Mathematical expressions for these indicators are presented in Equation 1-3, where  $F$  is the crushing force and  $\delta$  as the displacement [22].

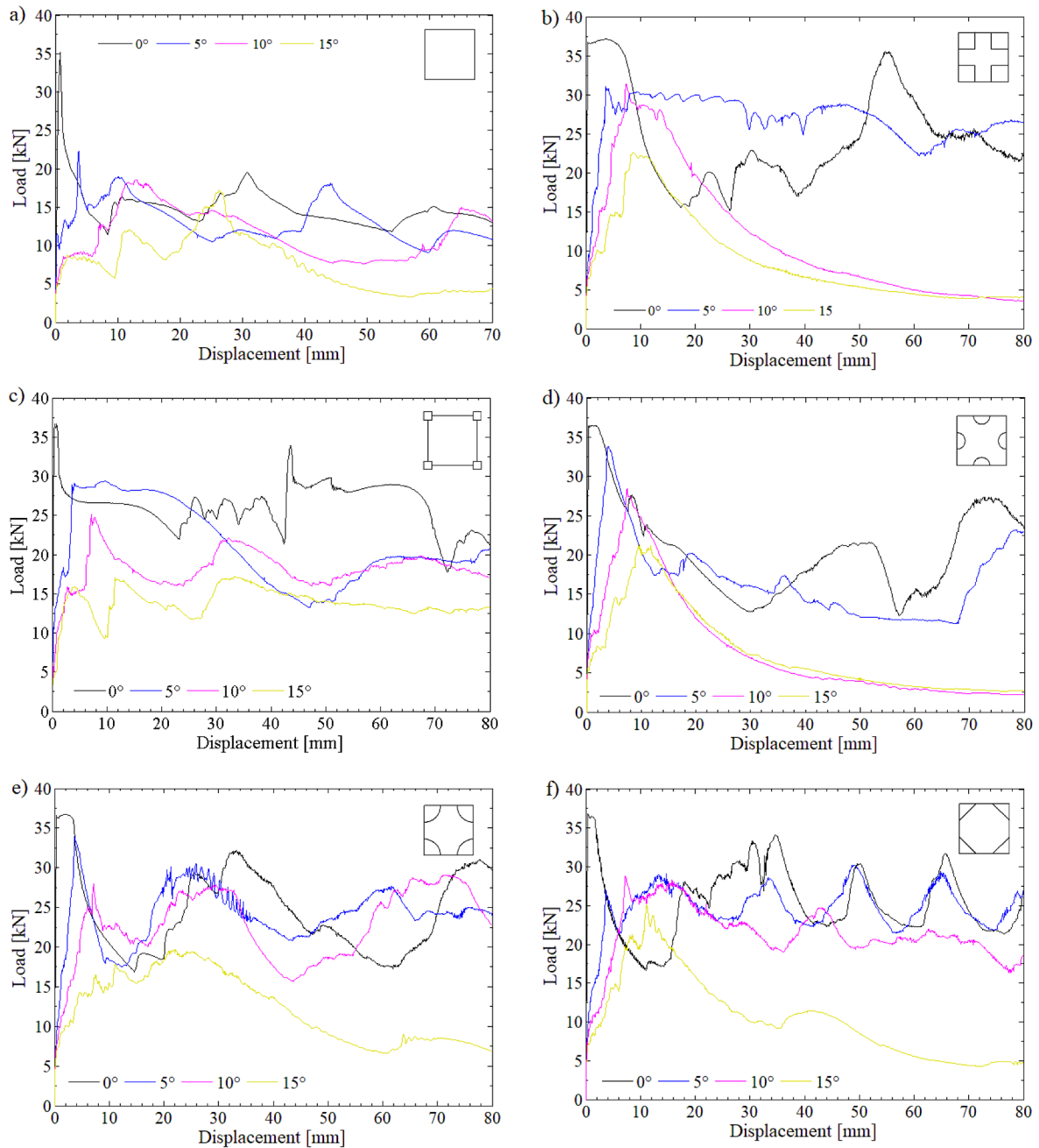


**Fig. 5.** Force vs displacement curves for all evaluated structures, where (a) ST-00, (b) MC-01, (c) MC-02, (d) MC-03, (e) MC-04, and (f) MC-05

$$E_a = \int_0^\delta F \cdot d\delta \quad (1)$$

$$P_m = E_a / \delta \quad (2)$$

$$CFE = P_m / P_{max} \quad (3)$$

To get a better understanding of the mechanical behavior of the peak load ( $P_{max}$ ) and the meaning force ( $P_m$ ) Figure 8 is presented. As possible to see, a peak load value close to 36 kN was achieved for all multicell structures and typical tube at  $0^\circ$ . As the loading angle increased, multicell structures reported better load-carrying

capacity concerning the ST-00 tube. However, a downward trend in  $P_{max}$  and  $P_m$  was observed in all structures, as the loading angle increased. The lowest  $P_{max}$  value equal to 17.19 kN was computed for structure MC-02, representing a decrease of 47.75% of this value, respect to its axial crushing condition. Keeping in mind that, the  $P_m$  is the mean force along the crushing process, all multicell structures exhibited a higher resistance to form the bulges than the typical square profile. Then higher values were obtained, which

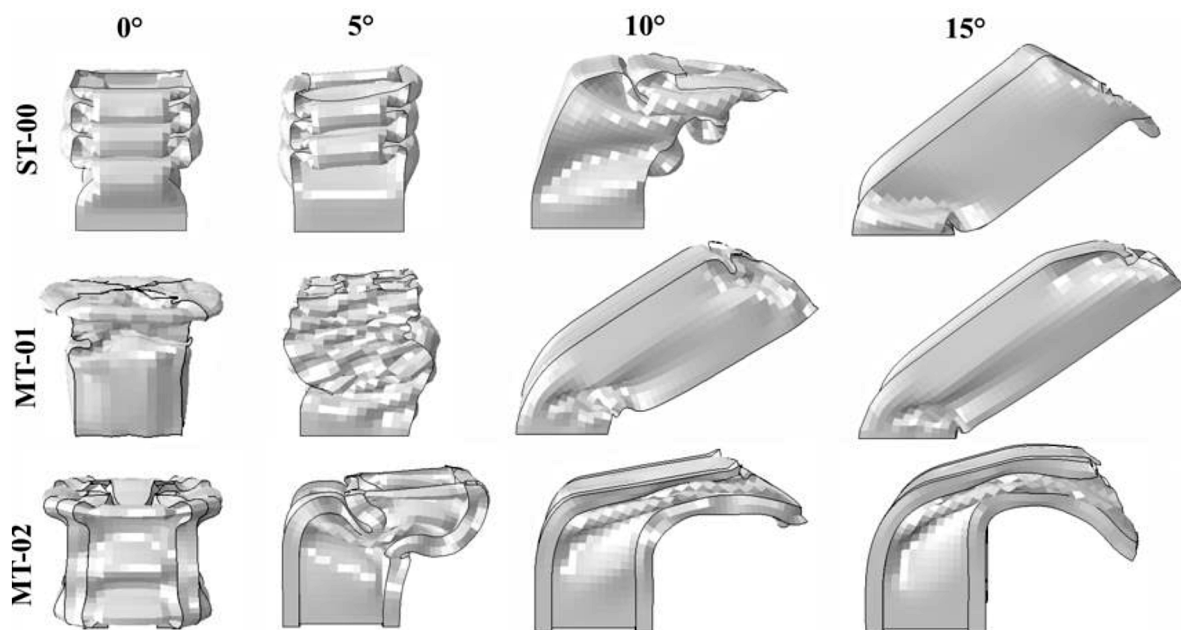


Fig. 6 Final deformation mode for evaluated structures at different  $\theta$  values, I

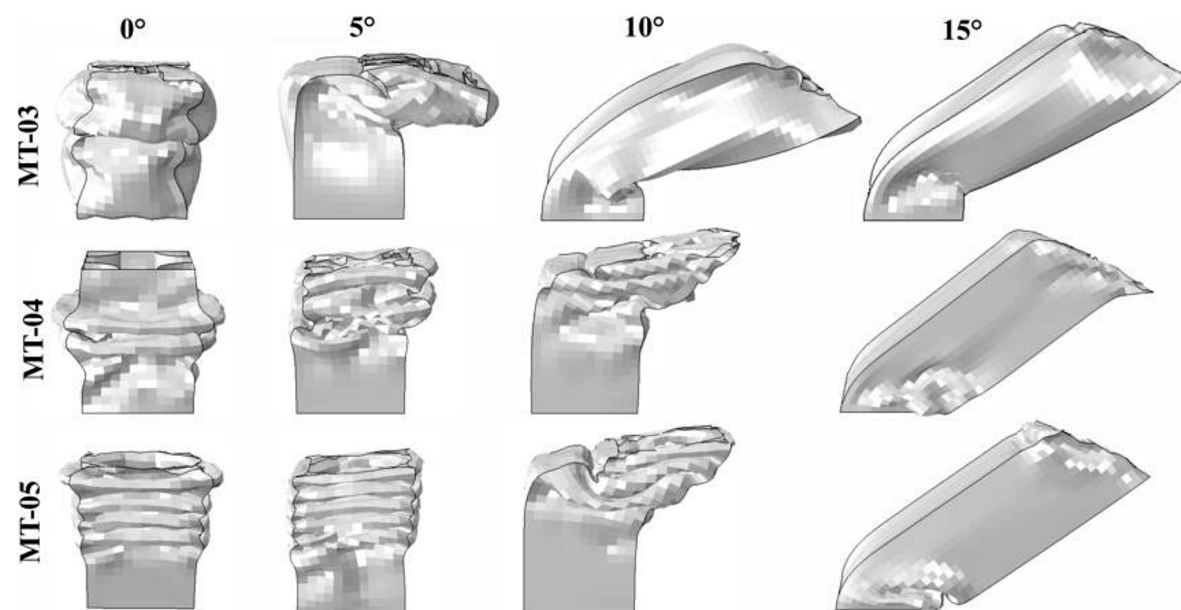


Fig. 7. Final deformation mode for evaluated structures at different  $\theta$  values, II

was most visible for  $\theta$  equal to 5 and 10°. The highest  $P_m$  value, ~26.82 kN was computed for a structure with a cross shape named MC-01 when loaded at 5°. The lowest  $P_m$  value was obtained for structure MC-03 at 15°, this value is low such as the lowest  $P_m$  for typical square tube.

With respect to energy absorbed ( $E_a$ ), this was calculated and plotted in Figure 8. As seen, the effectiveness of the multicell structures is corroborated since all structures improved their stability, which contributed to an increase in energy

absorption with respect to the ST-00 tube. In this way, for almost all loading angles, multicell structures increased their capacity to absorb energy by plastic deformation within a range from 3% to 104%. In all cases, the energy absorption decreased as the loading angle increased. According to the trend described, structures MC-2, MC-4 and MC-5 presented a better  $E_a$  performance regarding to the other multicell structures. The highest  $E_a$  value was achieved for structure MC-01 with 26.82 kN at 5° meanwhile the worst

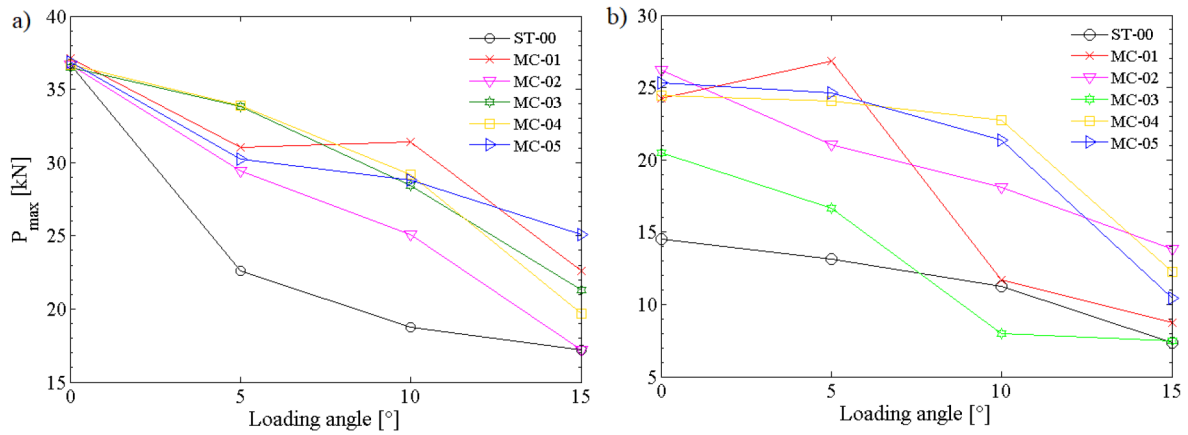


Fig. 8. (a) Pmax and (b) mean force (Pm) for all evaluated structures at different  $\theta$  values

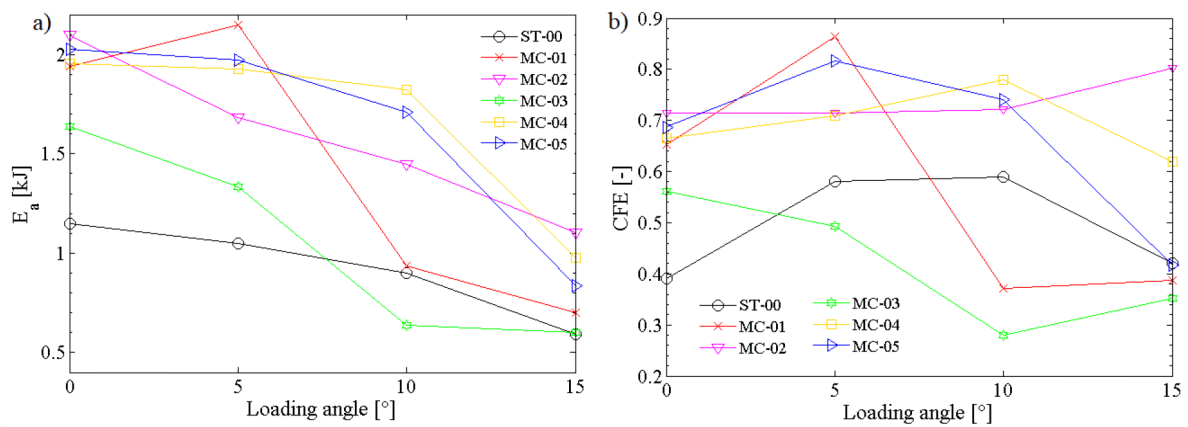


Fig. 9. (a) energy absorption and (b) crush force efficiency at different  $\theta$  values

behavior (0.28kJ) was computed for structure MC-03 at 10°. While the indicators presented above are important, in crashworthiness design, the crush force efficiency (CFE) is highly relevant. In this sense, an optimal value CFE is the unit indicating the optimum performance of the structure. For this indicator, two trends for multicell tubes were observed, the first trend was exhibited by the tubes MC-01, MC-03, and MC-05 where the CFE values varied greatly by changing the loading angle for the same structure. The second trend was described by the tubes MC-02 and MC-04, in this case, regardless of  $\theta$  values, the CFE was almost constant. Considering the CFE performance at different  $\theta$  values, the poorest behavior was obtained for structure with semicircles at mid-length on the side of the square (MC-03). In this case, CFE values comprised within 0.28-0.56 were computed. The highest CFE performance equal to 0.864 was achieved for structure MC-01 at  $\theta$  equal to 5°. However, considering that the structure should be effective at different

loading angles, the best CFE performance was achieved for structure MC-02, where an average CFE value of 0.74 was calculated.

Lastly, from the results presented above, the use of a multicell structure with small squares at the corners (MC-02) is highly recommended for controlling the crushing load at angles from 0° to 15°. Thus, this cross-section can serve as a baseline for engineers and designers in the design of energy absorption systems i.e. box crashes.

## CONCLUSIONS

In this work, a numerical study of the effect of loading angle ( $\theta$ ) on the crashworthiness performance of multicell structures was successfully performed. For this purpose, structures based on square cross-section were analyzed at different load angles such as 0°, 5°, 10° and 15°. Based on our numerical analysis, the following conclusions can be listed.

1. In general terms the square multicell structures exhibited a better crashworthiness performance regarding to square typical tubes.
2. Considering multicell structures, the geometric pattern plays an important role in the crashworthiness performance of the structures. In this sense, better stability was obtained in tubes MC-02, MC-04 and MC-05.
3. As the loading angle ( $\theta$ ) increases, a downward trend in Pmax, Pm, and Ea was observed in all structures. In this way, the Pmax value decreased by approximately 47.7% to be loaded from 0° to 15°.
4. The best energy absorption (Ea) performance was computed for structure MC-01 with 26.82 kN at 5°. This represents an improvement of 104% compared to the typical tube (ST-00) under the same load condition.
5. Considering the CFE indicator, the structure with the best performance at different load angles was the structure whose cross-section is a main square with smaller squares at the corners (MC-02). This tube had an acceptable and almost constant value of CFE close to 0.74. This value represents an improvement of CFE up to 51% compared to the typical square tube.
6. Lastly considering the last finding, structure MC-02 is widely recommendable to counter the harmful effects of crushing load not only at 0° but up to 15°. Thus, this cross-section could be used as a baseline for future designs of automobile components i.e crash bumpers.

## REFERENCES

1. Abdullah, N. A. Z., Sani, M. S. M., Salwani, M. S., & Husain, N. A. (2020). A review on crashworthiness studies of crash box structure. *Thin-Walled Structures*, 153, 106795.
2. Pei, T. S., Saffe, S. N. M., Rusdan, S. A., & Hamran, N. N. N. (2017). Oblique impact on crashworthiness. *International Journal of Engineering Technology and Sciences*, 4(2), 32-48.
3. Ferdynus, M., Rozylo, P., & Rogala, M. (2020). Energy absorption capability of thin-walled prismatic aluminum tubes with spherical indentations. *Materials*, 13(19), 4304.
4. Rogala, M., & Gajewski, J. (2023). Crashworthiness analysis of thin-walled square columns with a hole trigger. *Materials*, 16(11), 4196.
5. Tran, T., Hou, S., Han, X., Nguyen, N., & Chau, M. (2014). Theoretical prediction and crashworthiness optimization of multi-cell square tubes under oblique impact loading. *International Journal of Mechanical Sciences*, 89, 177-193.
6. Wang, W., & Qiu, X. (2017). An analytical study for global buckling of circular tubes under axial and oblique compression. *International Journal of Mechanical Sciences*, 126, 120-129.
7. Song, J., Xu, S., Zhou, J., Huang, H., & Zou, M. (2021). Experiment and numerical simulation study on the bionic tubes with gradient thickness under oblique loading. *Thin-Walled Structures*, 163, 107624.
8. Sun, G., Li, S., Li, G., & Li, Q. (2018). On crushing behaviors of aluminium/CFRP tubes subjected to axial and oblique loading: an experimental study. *Composites Part B: Engineering*, 145, 47-56.
9. Reddy, K. Y., Kumar, A. P., & Nagarjun, J. (2020). A computational study on the crushing behaviour of aluminium capped cylindrical tubes subjected to oblique load. *Materials Today: Proceedings*, 27, 1923-1927.
10. Pourseifi, M., & Bagherpoor, F. (2021). Numerical crushing analysis on energy absorption capability of a tapered corrugated composite tube under axial and oblique impact loading. *Waves in Random and Complex Media*, 1-22.
11. Karantza, K. D., & Manolacos, D. E. (2022). Crashworthiness analysis of square aluminum tubes subjected to oblique impact: Experimental and numerical study on the initial contact effect. *Metals*, 12(11), 1862.
12. Davoudi, M., & Kim, K. (2022). Energy Absorption Capability of Thin-Walled Structures with Various Cross Sections under Oblique Crash. *International Journal of Steel Structures*, 22(6), 1786-1797.
13. Zhang, H., Gao, Z., & Ruan, D. (2023). Square tubes with graded wall thickness under oblique crushing. *Thin-Walled Structures*, 183, 110429.
14. Liu, W., Jin, L., Luo, Y., & Deng, X. (2021). Multi-objective crashworthiness optimisation of tapered star-shaped tubes under oblique impact. *International journal of crashworthiness*, 26(3), 328-342.
15. Tian, K., Zhang, Y., Yang, F., Zhao, Q., & Fan, H. (2020). Enhancing energy absorption of circular tubes under oblique loads through introducing grooves of non-uniform depths. *International Journal of Mechanical Sciences*, 166, 105239.
16. Rogala, M., & Gajewski, J. (2021). Numerical analysis of porous materials subjected to oblique crushing force. In *Journal of Physics: Conference Series* (Vol. 1736, No. 1, p. 012025). IOP Publishing.
17. Li, W., & Fan, H. (2021). Crushing behavior of hierarchical hexagonal thin-walled steel tubes under oblique impact. *International Journal of Steel Structures*, 21, 202-212.
18. Alkhatib, S. E., Tarlochan, F., Hashem, A., & Sassi, S. (2018). Collapse behavior of thin-walled corrugated tapered tubes under oblique impact. *Thin-Walled*

- Structures, 122, 510-528.
19. Fan, D., Qi-hua, M., Xue-hui, G., & Tianjun, Z. (2021). Crashworthiness analysis of perforated metal/composite thin-walled structures under axial and oblique loading. *Polymer Composites*, 42(4), 2019-2036.
  20. ASTM INT (2004) ASTM E8/E8M - standard test methods for tension testing of metallic materials. *ASTM Int* (1):1–27.
  21. Zhang X, Zhang H, Wang Z (2016) Bending collapse of square tubes with variable thickness. *Int J Mech Sci* 106:107–116.
  22. Estrada, Q., Vergara-Vázquez, J., Szwedowicz, D., Rodriguez-Mendez, A., Gómez-Vargas, O. A., Partida-Ochoa, G., & Ortiz-Domínguez, M. (2021). Effect of end-clamping constraints on bending crashworthiness of square profiles. *The International Journal of Advanced Manufacturing Technology*, 116, 3115-3134.